Phase transitions in a forest-fire model

S. Clar, K. Schenk, and F. Schwabl
Institut für Theoretische Physik, Physik-Department der Technischen Universität München, James-Franck-Straβe, D-85747 Garching, Germany

(Received 11 July 1996; revised manuscript received 26 September 1996)

We investigate a forest-fire model with the density of empty sites as a control parameter. The model exhibits three phases, separated by one first-order phase transition and one ''mixed'' phase transition which shows critical behavior on only one side and hysteresis. The critical behavior is found to be that of the self-organized critical forest-fire model [B. Drossel and F. Schwabl, Phys. Rev. Lett. **69**, 1629 (1992)], whereas in the adjacent phase one finds the spiral waves of the Bak, Chen, and Tang forest-fire model [P. Bak, K. Chen, and C. Tang, Phys. Lett. A **147**, 297 (1990)]. In the third phase one observes clustering of trees with the fire burning at the edges of the clusters. The relation between the density distribution in the spiral state and the percolation threshold is explained and the implications for stationary states with spiral waves in arbitrary excitable systems are discussed. Furthermore, we comment on the possibility of mapping self-organized critical systems onto ''ordinary'' critical systems. [S1063-651X(97)04502-9]

PACS number(s): 64.60.Lx, 05.70.Jk, 05.70.Ln

I. INTRODUCTION

In 1990, Bak, Chen, and Tang introduced a simple model for the spreading of a fire in a forest or the spreading of disease in a population [1]. The individuals (sites on a square lattice in two dimensions) can be in one of three states: tree (healthy, excitable), tree on fire (infected, excited), and ashes or empty site (immune or dead, refractory). New individuals are ''fed'' into the system with a small rate p. Whether the third state is considered as death of an individual and p consequently as the birth rate of new individuals, or as a state of immunity, and $1/p$ as the time scale of the loss of that immunity, is a matter of interpretation. In the following, we will use the terms tree, fire, empty site, and refer to p as the tree growth rate. The exact rules of the model [1] were as follows: (i) at each time step trees grow at empty sites with a small probability p, (ii) trees on fire will burn down at the next time step and turn to empty sites, (iii) the fire on a site will spread to the trees at its nearest-neighbor sites at the next time step. Although originally claimed to be critical in the limit $p \to 0$, the simulations in [2,3] showed that the model does not display criticality. Instead, one could observe quasideterministic spiral waves of fires.

In 1992, Drossel and Schwabl introduced the self-organized critical forest-fire model (SOC FFM) [4] with an additional rule: (iv) if no nearest neighbor is burning, a tree catches fire with a small ''lightning'' probability f. Under the condition of a double separation of time scales [time between two lightning strokes $1/f \gg$ (time scale of tree growth) $1/p \gg$ (time needed to burn down large tree clusters)] the model shows critical behavior over a wide range of parameter values. The properties of this model were investigated in, e.g., [5–8].

In this paper, we shall investigate a model with the same type of interactions while keeping constant the number of empty sites or immune individuals. Their density is the control parameter of the model. Parameters like p or f do not enter the model. We will show that the model exhibits three phases, two of which can be shown to display the same behavior as the above mentioned models. The third phase shows clustering of trees with the fire burning at the edges of the clusters.

In the ''spiral-wave'' phase, which exists not only in this model, but in a large number of excitable systems (for a review on excitable systems see, e.g., [9,10]), we will point out an interesting relation to the nonequilibrium percolation model of [11]. There, the tree density was the control parameter and the following rules were iterated: (i) Lightning strikes an arbitrary site in the system. If the site is occupied, the whole cluster of s trees, which is connected to this site (by nearest-neighbor coupling), burns down, i.e., the trees of this cluster turn to empty sites. (ii) Then s new trees are grown at randomly chosen empty sites (including the ones that have just turned empty). The close relation between this model and the model treated in the present paper will enable us to identify the mechanism that determines the density distribution of excitable constituents and, in particular, the density immediately in front of excitation fronts in the spiral-wave phase of excitable systems.

Furthermore, the model presented in this paper, as well as the model in [11], are examples of reformulations of a SOC model in terms of a control parameter (the density of trees or empty sites, respectively). Both models indicate that the claim in [12] that all SOC models can be mapped onto ordinary critical systems exhibiting a subcritical phase, a critical phase with a smoothly varying order parameter and a critical point that separates the two phases, is not true in general. Nonequilibrium systems and their phase transitions show a much richer behavior than equilibrium systems, with many features that are unknown in equilibrium.

II. THE MODEL

The model is defined on a d-dimensional hypercubic lattice with L^d sites. If not stated otherwise, we choose $d=2$ and periodic boundary conditions in the following. $\rho_e L^d$ sites are randomly chosen to be empty. The density of empty sites ρ_e is the control parameter of the model. The remaining sites

are randomly filled with trees and fires. Their densities are denoted by ρ_t and ρ_f. It is always $\rho_t+\rho_e+\rho_f=1$. The exact values of ρ_t and ρ_f in the initial state do not affect the stationary state, except in the vicinity of certain points which will be discussed later.

The system is iterated as follows: (i) all trees on fire will burn down the next time step, (ii) the fire on a site will spread to the trees at its nearest-neighbor sites in the next time step, (iii) after each time step the same number of trees that have burnt down grow at randomly chosen empty sites (including the ones which have just become empty), thereby keeping ρ_e fixed, and (iv) if the fire dies out, a randomly chosen tree catches fire spontaneously.

The motivation of rule (iv) is the following: We want to investigate the system under the action of a vanishingly small lightning probability. Since the process which is described by rule (iv) may then take very long in real time, but nevertheless can be simulated in one iteration step, rule (iv) represents an acceleration of the real process. When calculating temporal averages of the fire density, this point has to be considered.

The reason for choosing the density of empty sites as parameter and not the density of trees is the following: Consider a system that consists only of trees and replace one tree by a fire. In the next step we have four fires, but only one empty site to grow new trees. This extreme example shows that there might be situations in which it is not possible to keep the density of trees constant. The density of empty sites, in turn, can always be kept constant for arbitrary values within the interval [0,1].

In the following sections, we discuss the properties of the stationary state as function of the density of empty sites ρ_e. In Sec. III, we start with a high density of empty sites and investigate the region of vanishing fire density. In Sec. IV, we lower the density of empty sites which leads to a state with spiral waves. A detailed description of the mechanism which determines the density distribution in the spiral state is given in Sec. V. Section VI investigates the more homogeneous, ''mixed'' phase that can be observed after further decreasing the density of empty sites. Up to here, only two-dimensional square lattices are considered. Section VII treats other dimensions and lattice types. In Sec. VIII, we comment on the issue of mapping self-organized criticality onto ordinary criticality. Finally, in the Appendix, we present some general properties of the order parameter curve.

III. REGION OF VANISHING FIRE DENSITY AND CRITICAL POINT

For $\rho_e \lesssim 1$, there exist only very small tree clusters, and, consequently, if one starts a fire by setting on fire a randomly chosen tree, it soon dies out, and one has to start a new one. The average number of trees $\overline{s}$ destroyed by a fire therefore is finite and small, and in the thermodynamic limit $L\to\infty$ the fire density ρ_f equals zero (taking into account that rule (iv) is an acceleration of a process which takes infinitely long in real time). In our simulations the maximum system size was 6000^2. With decreasing ρ_e, $\overline{s}$ increases, but still remains finite, and therefore $\rho_f=0$. If ρ_e is decreased further, we finally arrive at a critical density $\rho_e^{c,1}\approx 59.2\%$ ($\rho_t^{c,1}=1-\rho_e^{c,1}\approx 40.8\%$), where $\overline{s}$ diverges with a power law $\overline{s}\propto(\rho_e-\rho_e^{c,1})^{-\delta}$, with some exponent δ. A snapshot of the system in the vicinity of $\rho_e^{c,1}$ is shown in Fig. 1.

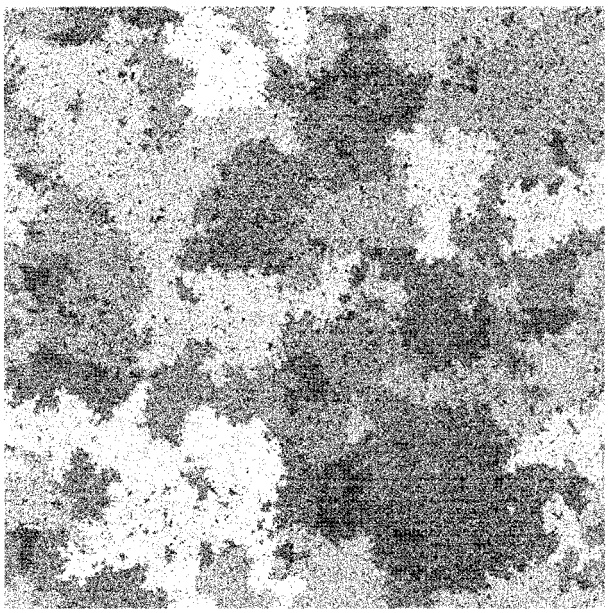

FIG. 1. Snapshot of the stationary state in the ''SOC'' phase near the critical density $\rho_e^{c,1}\approx 59.2\%$. $L=2000$ and $\rho_e=59.8\%$. Trees are black and empty sites are white.

The critical behavior close to $\rho_e^{c,1}$ can be described by exponents which are defined as in percolation theory [13]. The size distribution of tree clusters is $n(s)\propto s^{-\tau}\mathcal{C}(s/s_{\max})$ with a cutoff function $\mathcal{C}$. $s_{\max}$ is the size of the largest cluster in the system and diverges for $\rho_e\to\rho_e^{c,1}$. The fractal dimension μ of the clusters is defined by $R(s)\propto s^{1/\mu}$, where R is the radius of gyration of a cluster. The correlation length is given by $\xi\propto(\rho_e-\rho_e^{c,1})^{-\nu}$. More exponents can be defined and scaling relations between them can be derived (see, e.g., [5–8]).

The critical exponents found in the simulations [$\tau=2.14(4)$, $\mu=1.95(2)$, and $\nu=0.28$] are the same as in the SOC FFM, when appropriately redefined (for ν one has to change variables from f/p to ρ_e via $\rho_e-\rho_e^{c,1}\propto(f/p)^{1/\delta}$ (see [8])). Also the critical density $\rho_t^{c,1}\approx 40.8\%$ remains the same. This model displays exactly the same critical behavior as the SOC FFM and the model of [11], because in a system which is much larger than the correlation length, neither the difference between a globally conserved density ρ_e (this model and [11]) and a density ρ_e, which is only conserved on an average (SOC FFM), nor the difference between instantaneous regrowth of trees (this model) or delayed regrowth (SOC FFM and [11]) can be seen on length scales comparable to the correlation length.

In the stationary state of the SOC FFM $\overline{s}=p\rho_e/f(1-\rho_e)$, since in one time step there are $\rho_t L^d f$ lightning strokes and $\rho_e L^d p$ new trees are growing. Therefore, if we measure in our model $\overline{s}$ for a certain value of the control parameter ρ_e we know that its behavior is that of the SOC FFM for $f/p=\rho_e/\overline{s}(1-\rho_e)$.

IV. REGION OF FINITE FIRE DENSITY I: SPIRALS

If we decrease the number of empty sites beyond the critical point $\rho_e^{c,1}$ the size of the largest forest cluster diverges,

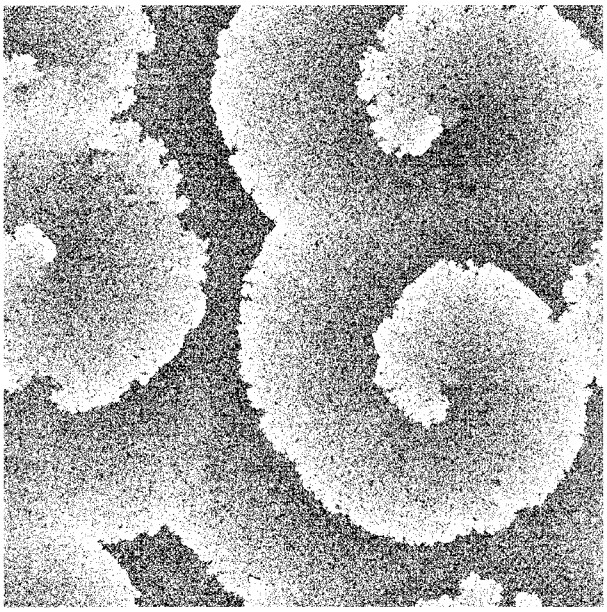

FIG. 2. Snapshot of the stationary state in the ''spiral-wave'' phase for $L=1000$ and $\rho_e=59\%$. Trees are gray and empty sites are white. The fires are black, but difficult to see. They are located at those lines where the density of trees changes abruptly.

and we would expect the fire not to be extinguished any more. Therefore, one might expect the fire density ρ_f to behave as an order parameter that sets in at $\rho_e^{c,1}$ and grows smoothly from zero to finite values, obeying some power law $\rho_f \propto (\rho_e^{c,1}-\rho_e)^{\beta}$. Instead, the following behavior can be observed in the simulations: The system restructures, fires gathering to form spirals and the regions of different densities (see Fig. 1) vanishing in favor of a smooth density distribution between the spiral arms (see Fig. 2). The behavior of the spirals is quasideterministic. Immediately in front of the fire fronts the tree density is very high and immediately behind them it is very low. The density distribution is treated in more detail in Sec. V. The distance Δ between two spiral arms is finite and constant throughout the system. The fire density for $\rho_e=\rho_e^{c,1}-0$ is also finite. Decreasing ρ_e further, the distance between the spiral arms becomes smaller and the fire density becomes larger, since it is now easier for the fire to survive. At $\rho_e=\rho_e^{c,3}\approx 54.2\%$, the spiral state breaks down and another restructuring to a new phase takes place, which will be treated in Sec. VI.

For $\rho_e \leqslant \rho_e^{c,1}$ the fire is able to sustain itself and it is no longer necessary to keep it alive by setting on fire randomly chosen trees each time the fire has died out. The ''external field'' can be set zero. In terms of tree growth and lightning, we have a model with tree growth rate p, but without lightning rate f. Therefore, the behavior in the spiral state at some density ρ_e is exactly the same as in the forest-fire model of Bak, Chen, and Tang in [1] for a certain value of the tree growth probability p, since in the thermodynamic limit it does not matter which of the variables is kept fixed. The fluctuations of the densities in the Bak model vanish for $L\to\infty$, as do the fluctuations of the number of new grown trees per time step in this model.

In the Bak model, one observes a diverging distance between spiral arms for $p\to 0$. If we start in our model with a spiral state and increase ρ_e beyond $\rho_e^{c,1}$ (corresponding to a decrease of p), the system does not undergo a phase transition at $\rho_e=\rho_e^{c,1}$, but chooses to retain the spiral state up to $\rho_e=\rho_e^{c,2}\approx 60.8\%$. This value of ρ_e with $\Delta=\infty$ corresponds to $p=0$ in the Bak model. As function of p the order parameter follows the power law $\rho_f \propto p$ (see the explanation in Sec. V).

As already found in [2,3], the spiral state does not display criticality or scale invariance in the sense of clusters or events on all length scales. For a particular value of p the model does not show events on all scales, but only on the scale $1/p$, and behaves essentially deterministic. However, the model allows similarity transformations, since a system with parameter p_1 can be obtained by rescaling a system with parameter p_2.

What we have found is a discontinuous phase transition which is neither of first nor of second order. We find hysteresis (the state of the system for a density in the interval $[\rho_e^{c,1};\rho_e^{c,2}]$ depends on from which side one approaches this region), an order parameter that increases smoothly from zero at $\rho_e^{c,2}$ to finite values, and critical behavior on only one side of the transition ($\rho_e \geqslant \rho_e^{c,1}$, the side with vanishing order parameter). The order parameter curve for a two-dimensional system is shown in Fig. 3.

The reason why the critical point $\rho_e=\rho_e^{c,1}$ is not an ordinary critical point is the same as in [11]. From Fig. 1, it can be seen that, in addition to large tree clusters, there exist also large clusters of empty sites. In contrast to ordinary critical phenomena (e.g., percolation), there is no homogeneously distributed set of large clusters that could join at $\rho_e=\rho_e^{c,1}$ to form an infinite cluster that spans the whole system. Rather, the largest cluster has to compete with all other regions with different densities (which, due to the very nature of the dynamics, are nothing more than different growth stages of the largest cluster itself) for space in the system. Or, to put it differently, an infinite cluster, like in percolation, is impossible, because the system has to provide space not only for the infinite cluster, but also for a large number of ''younger'' copies of it. The violation of the hyperscaling relation $d=\mu(\tau-1)$ also indicates the inhomogeneous distribution of density in the forest-fire model. As explained in [5], the violation is equivalent to the statement that not every part of the system contains a spanning cluster at criticality.

V. DENSITY DISTRIBUTION IN THE SPIRAL STATE

In order to better understand the density distribution in the spiral state, we shall now investigate a state with a single front propagating through a square system with periodic boundary conditions (see the left side of Fig. 4). Since this can be considered to be a section of a spiral state (see the right side of Fig. 4), and the spiral state, in turn, can be completely covered by such sections (if the edge length is chosen to be equal to the distance Δ between two successive arms of the spirals), it is sufficient to understand the density distribution in this part of the whole system. Instead of successive fire fronts passing through the small section of the system, one might also think of a single fire front which repeatedly leaves the section at one end and reenters at the

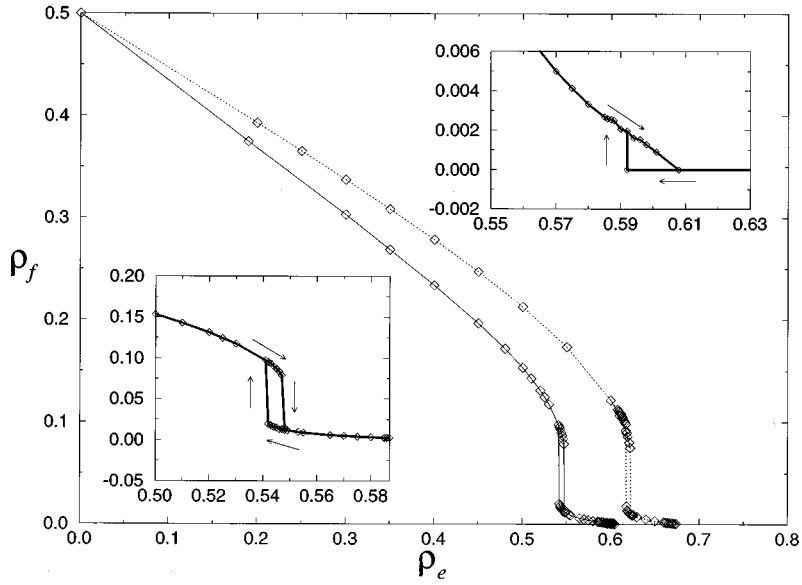

FIG. 3. The order parameter fire density ρ_f as function of the density of empty sites ρ_e in two dimensions (—, square lattice; . . . , triangular lattice). The magnified sections in the insets show the two transitions of the two-dimensional system on a square lattice. To the left, one can see the first-order phase transition at $\rho_e^{c,3}$ and $\rho_e^{c,4}$ between the mixed phase and the spiral phase, and to the right the ''mixed'' phase transition at $\rho_e^{c,1}$ and $\rho_e^{c,2}$ between the spiral phase and the SOC phase. The arrows indicate the directions in which the transitions are traversed.

other end due to periodic boundary conditions.

The tree density immediately in front of the fire front ρ_t^{before} has to be larger than or equal to the percolation threshold for site percolation on a square lattice $p_c \approx 0.59$, for otherwise there would not be propagation. With increasing distance from the fire front, the tree density smoothly decreases, until one finally arrives again on the other side of the front, where the density takes its lowest value ρ_t^{after}. If ρ_t^{before} was exactly the percolation threshold, the fire would burn down a vanishing fraction of all trees, and the propagation speed of the front would be zero. The densities in front of and behind the fire front would be equal ($\rho_t^{\text{before}} = p_c = \rho_t^{\text{after}}$), as claimed in [2]. However, the simulations clearly show that this is not the case. ρ_t^{before} is higher than the percolation threshold, the density ρ_t^{after} in a region after the fire has passed through it is very low, but not equal to zero, and the propagation speed of the fire fronts v_{fire} is nonvanishing (0.7 ± 0.05 site per iteration step near $\rho_e^{c,2}$). What is the mechanism that determines the density distribution and the values of the density immediately in front of and behind the fire front?

We shall approximate the periodic ''single front'' state even further by a coarsened state with a finite but large number n of stripes of equal width and different densities parallel to the fire front. Each stripe has homogeneous density. Let $\rho_t^1, \ldots, \rho_t^n$ be the densities of the n stripes, starting with the highest density. ρ_t^i is then the average density of the original smooth ''single front'' system in the region covered by the ith stripe ($\rho_t^1 \approx \rho_t^{\text{before}}$ and $\rho_t^n \approx \rho_t^{\text{after}}$). We also coarsen time, in that we consider the propagation of the fire front from the bottom of one stripe to its top as one time step. Growing of new trees then takes place after each (coarsened) time step. If one sets on fire the baseline of the stripe with highest density, the infinite cluster in that stripe will surely be set on fire, since it has many connections with the baseline, and the propagation of the fire front effectively causes the removal of the infinite cluster from this stripe.

The propagation of the fire front therefore can be modeled as follows. First, we identify the infinite cluster in the stripe with highest density and remove it from the system. Doing this one has to respect the boundaries of the stripes, although the infinite cluster of course extends into the neighboring stripes. The strength of the infinite cluster at density ρ_t^1 is denoted $P(\rho_t^1)$. [We now define also the density ρ_t^{n+1} of the stripe which contained the infinite cluster after its removal, i.e., $\rho_t^{n+1} = \rho_t^1 - P(\rho_t^1)$.] Second, the $P(\rho_t^1)\Delta^2/n$ trees of the infinite cluster are redistributed randomly amongst the empty sites of the whole system of size Δ^2. If the system is to be stationary, the stripes thereby just exchange their densities, i.e., the stripe with second highest density ρ_t^2 now assumes the highest density ρ_t^1, and so on. From that condition, one can easily derive the equation

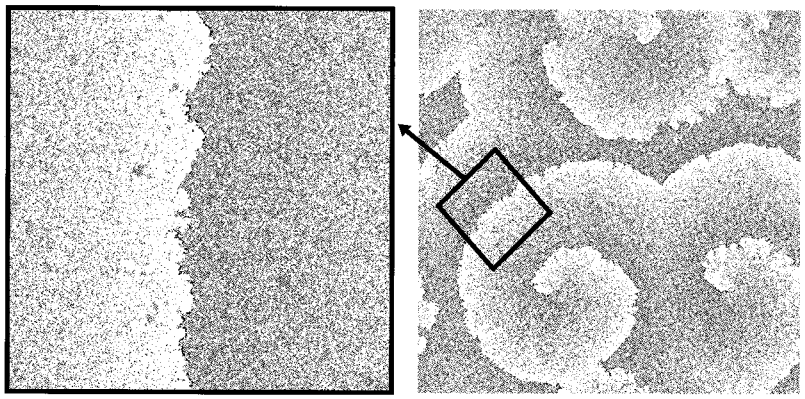

FIG. 4. A spiral state at density $\rho_e = 59\%$ with distance Δ between successive fire fronts can be covered by quadratic ''single front'' sections of edge length Δ. Trees are gray, fires are black, and empty sites are white.

$$\rho_t^{i-1}=\rho_t^i+(\rho_t^1-\rho_t^{n+1})(1-\rho_t^i)/[n(1-\rho_t)+\rho_t^1-\rho_t^{n+1}]$$

for $i=2,\ldots,n+1$. The last factor on the right-hand side represents the fraction of trees of the infinite cluster that are regrown in the stripe with density ρ_t^i. We finally obtain

$$\frac{1-\rho_t^1}{1-\rho_t^2}=\frac{1-\rho_t^2}{1-\rho_t^3}=\cdots=\frac{1-\rho_t^n}{1-\rho_t^{n+1}}. \tag{1}$$

Together with $\rho_t=(1/n)\Sigma_{i=1}^n\rho_t^i$ we have n equations for $n+1$ densities. These equations were already derived in [11] for a related model. The average density in a system with n stripes is then

$$\rho_t=1-\frac{1-\rho_t^{n+1}}{n}\sum_{i=1}^{n}\left(\frac{1-\rho_t^1}{1-\rho_t^{n+1}}\right)^{i/n}$$

$$=1-\frac{\rho_t^1-\rho_t^{n+1}}{n\{[(1-\rho_t^1)/(1-\rho_t^{n+1})]^{-1/n}-1\}}.$$

In the system that we are really interested in, the density varies smoothly, so we have to consider large n. In [11] it was argued that ρ_t^1 has always to be greater than or equal to a certain constant $\rho_t^*\approx 0.625>p_c$. If this were not the case, a traversing fire front would leave behind large tree clusters which would lead to inhomogeneities that prevented the next fire front from passing through in the same quasideterministic way than the first one. Likewise, ρ_t^{n+1} has always to be greater than or equal to another constant $\rho_t^\infty=\rho_t^*-P(\rho_t^*)\approx 0.078$. ρ_t^* is always larger than the corresponding percolation threshold p_c. These constants have a more fundamental significance independently of this model and of any states with spiral waves (for details see [11,14]). The case $\rho_t^1=\rho_t^*$ and $\rho_t^{n+1}=\rho_t^\infty$ corresponds to the lowest possible overall density and therefore to the state with infinite spirals at $p=0$ or $\rho_e=\rho_e^{c,2}$. In this case, we have $\rho_t^{\text{before}}=\rho_t^*$ and $\rho_t^{\text{after}}=\rho_t^\infty$.

The overall density in the spiral state can then be written as

$$\rho_t=1-\frac{\rho_t^{\text{before}}-\rho_t^{\text{after}}}{\lim_{n\to\infty}n\left[\left(\frac{1-\rho_t^{\text{before}}}{1-\rho_t^{\text{after}}}\right)^{-1/n}-1\right]}$$

$$=1-\frac{\rho_t^{\text{before}}-\rho_t^{\text{after}}}{\lim_{n\to\infty}n\left[1-\ln\left(\frac{1-\rho_t^{\text{before}}}{1-\rho_t^{\text{after}}}\right)\Big/\ n\pm\cdots-1\right]}$$

$$=1-\frac{\rho_t^{\text{before}}-\rho_t^{\text{after}}}{\ln\left(\frac{1-\rho_t^{\text{after}}}{1-\rho_t^{\text{before}}}\right)}. \tag{2}$$

For $\rho_t^{\text{before}}=\rho_t^*$ and $\rho_t^{\text{after}}=\rho_t^\infty$, this density should be equal to the density $\rho_t^{c,2}$ of the state with spirals of infinite extension. With the values of ρ_t^* and ρ_t^∞ measured in [11] (0.625 and 0.078 for the square lattice, 0.533 and 0.062 for the triangular lattice), one arrives at $\rho_t^{c,2,\text{calculated}}=0.392\pm0.002$ for the square lattice and $\rho_t^{c,2,\text{calculated}}=0.325\pm0.002$ for the triangular lattice, in excellent agreement with the values $\rho_t^{c,2}=0.392\pm0.002$ for the square lattice and $\rho_t^{c,2}=0.323\pm0.005$ for the triangular lattice, measured in the spiral state of this model.

Since Eq. (1) represents a geometric series, the density as function of the distance from the fire front is given by

$$\rho_t(x)=1-(1-\rho_t^{\text{after}})\left(\frac{1-\rho_t^{\text{before}}}{1-\rho_t^{\text{after}}}\right)^{x/\Delta}, \tag{3}$$

with $\rho_t(0)=\rho_t^{\text{after}}\gtrsim\rho_t^\infty$ and $\rho_t(\Delta)=\rho_t^{\text{before}}\gtrsim\rho_t^*$

With our new knowledge about the nature of the spiral state, we can derive an equation for the distance Δ between the fire fronts as function of the tree growth probability p. Let the speed of the fire fronts $v_{\text{fire}}(\rho_t^{\text{before}})$ be measured in sites per iteration step. Like P it depends on the density in front of the fire front ρ_t^{before}. The amount of matter burnt in unit time is then $P(\rho_t^{\text{before}})v_{\text{fire}}(\rho_t^{\text{before}})\Delta$. This has to be equal to the number of growing trees per unit time $(1-\rho_t)p\Delta^2$, leading to the relationship

$$\Delta=\frac{P(\rho_t^{\text{before}})v_{\text{fire}}(\rho_t^{\text{before}})}{1-\rho_t}\frac{1}{p}. \tag{4}$$

This confirms the observed scaling behavior $\Delta\propto p^{-1}$ and additionally delivers the constant of proportionality, being 0.63 ± 0.05 for $\rho_t^{\text{before}}=\rho_t^*$ and in good agreement with the simulations. Since the fire density is inversely proportional to the distance between the spiral arms, we find $\rho_f\propto p$, i.e., the order parameter exponent β equals one. This can also be seen from the equality $\rho_f=p\rho_e$ [15], which states that the number of burnt trees has to be equal to the number of new grown trees in the stationary state.

If one chooses a fixed site behind the front and wants to know the tree density in this region as function of the time t until at $T=\Delta/v_{\text{fire}}$ the next front passes through, one has to replace in Eq. (3) x by $v_{\text{fire}}t$ and arrives with Eq. (4) at

$$\rho_t(t)=1-(1-\rho_t^{\text{after}})\left[\left(\frac{1-\rho_t^{\text{before}}}{1-\rho_t^{\text{after}}}\right)^{[(1-\rho_t)/P(\rho_t^{\text{before}})]}\right]^{pt},$$

which with Eq. (2) and $P(\rho_t^{\text{before}})=\rho_t^{\text{before}}-\rho_t^{\text{after}}$ leads to

$$\rho_t(t)=1-(1-\rho_t^{\text{after}})e^{-pt}. \tag{5}$$

Equation (5) can also be derived easily from $\partial\rho_t/\partial t=p(1-\rho_t)$, first stated in [2]. This shows that our picture is in accordance with the basic equations describing the spiral state.

One additional point concerning Eq. (4) should be mentioned. Equation (4) relates Δ, ρ_t, and p. If one regards, e.g., Δ as fixed, only the product $(1-\rho_t)p$ is determined. This reflects the fact that in a ''single front'' state with fixed edge length Δ one can have different overall densities ρ_t. The other quantities adjust themselves automatically. However,

in the ''real'' spiral state, fixing Δ determines invariably all other quantities. Since the spiral state can be constructed by connecting ''single front'' systems, this seems to be a contradiction. The solution of this apparent contradiction is that one has neglected the spiral centers. They yield a second, unfortunately unknown, relation between Δ, ρ_t, and p. This relation is brought about by the rotation of the spiral centers. ρ_t and p determine the angular velocity ω of the rotation, which, in turn, determines Δ via $\Delta = v_{\text{fire}} T = v_{\text{fire}} 2\pi/\omega$. For the calculation of $\rho_t^{c,2}$ with Eq. (2), using the decomposition into ''single front'' states, it is justified to neglect the spiral centers, because in the thermodynamic limit their number density is zero. Nevertheless, one has to be aware of the fact that, although not important for calculating $\rho_t^{c,2}$, the spiral centers are the ''pacemakers'' of the spirals and therefore responsible for the magnitude of Δ.

Another interesting point is that the density $\rho_e^{c,2}$ can also be found from an extremum principle first stated in [4]. There, the extremum principle was erroneously used to determine the critical density $\rho_t^{c,1}$ of the SOC FFM. The fire was believed to destroy as many trees as it can at the critical point, but the result $\approx 39\%$ was in contradiction to the measured value $\rho_t^{c,1} \approx 40.8\%$ [5–8]. However, the equations derived in [4] from the extremum principle can easily be seen to be equivalent to Eq. (2) for the spiral state. Therefore, the principle yields the correct critical density, but for a different, then unknown, phase of the model.

From the results found in this section one can draw some conclusions for excitable media in general. In many excitable systems stationary states with spiral waves can be found. Famous examples are, e.g., the Belousov-Zabhotinski (BZ) reaction [16] or the electrophysiological activity of heart tissue [17]. If the spirals are to sustain themselves in a stationary state, the density of the excitable constituents (the ''fuel'') in a region immediately before a fire front passes through it ρ_t^{before} has always to be larger than or equal to some threshold ρ_t^*, which, in turn, is larger than the percolation threshold p_c for that particular situation. The percolation threshold can, in principle, be measured by preparing a homogeneous system with a certain density of excitable constituents and ''exciting'' one edge of the system. If the resulting excitation front dies out before reaching the other end of the system, we are still below the percolation threshold, and if it reaches the other end in finite time we are above. At the percolation threshold the front barely survives and needs an infinitely long time to reach the other end. The overall density of the excitable constituents has to be above the value $\rho_t^{c,2}$, below which no excitation can be sustained.

A system that displays spiral waves or avalanches (concentric waves, target patterns) depending on the density of excitable constituents are, e.g., populations of dictyostelium discoideum amoebae [18]. There, circular waves of signaling activity emanating from pacemakers are found for low cell densities, whereas for high cell densities one observes spiral waves.

VI. REGION OF FINITE FIRE DENSITY II: THE MIXED PHASE

With decreasing ρ_e, the distance between the spiral arms becomes smaller and the spirals finally break up to single fronts. This change occurs continuously. The fronts, which are more irregular than the spirals, have also been observed in the model of Bak, Chen, and Tang. Decreasing ρ_e further, the coherence length of the fronts soon becomes comparable with the lattice constant, and the system reorganizes itself discontinuously into another state, which constitutes the third phase of this model. This happens at $\rho_e = \rho_e^{c,3} \approx 54.2\%$. The simulations show that the trees in the new state tend to ''cluster'' (to form regions with higher tree density) with the fire burning at their edges (see Fig. 5). To sustain this type of structure, a certain minimum density of fires is needed. At $\rho_e = \rho_e^{c,3}$, ρ_f jumps from 2% to 10%. If one lowers ρ_e further, the size of the ''clusters'' decreases, and the fire density increases. The system as a whole becomes more homogeneous (trees, fires, and empty sites are ''mixed''). For $\rho_e = 0$, we observe $\rho_t = \rho_f = 1/2$ for all dimensions and lattice types. The order parameter curve starts linearly at $\rho_e = 0$ with a slope that depends only on the number of nearest neighbors z (see the explanations in the Appendix). If we start with small ρ_e and traverse the phase transition in the other direction, it takes place at different ρ_e ($\rho_e^{c,4} \approx 54.7\% > \rho_e^{c,3}$), i.e., one has a first-order phase transition with hysteresis. The order parameter as function of the density of empty sites is shown in Fig. 3.

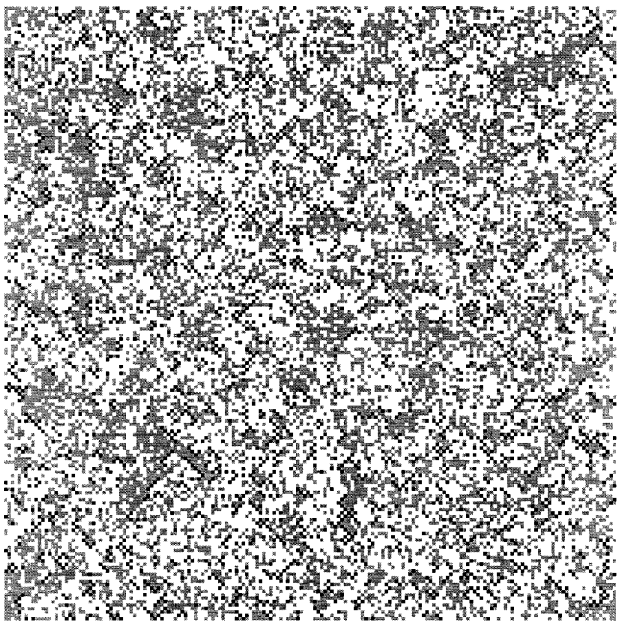

FIG. 5. Snapshot of the stationary state in the ''mixed'' phase near the critical density $\rho_e^{c,4} \approx 54.7\%$. $L = 180$ and $\rho_e = 54.6\%$. Trees are gray, fires are black, and empty sites are white.

VII. DIMENSIONS OTHER THAN TWO AND DIFFERENT LATTICE TYPES

Since in one dimension there cannot exist spiral waves, we expect a simpler phase diagram than in two dimensions. For $\rho_e = 0$ we are dealing with a completely deterministic one-dimensional cellular automaton where each site can be in one of two states (automaton no. 54, according to the classification scheme of Wolfram [19]). In the stationary state each tree has at least one fire as a neighbor and vice

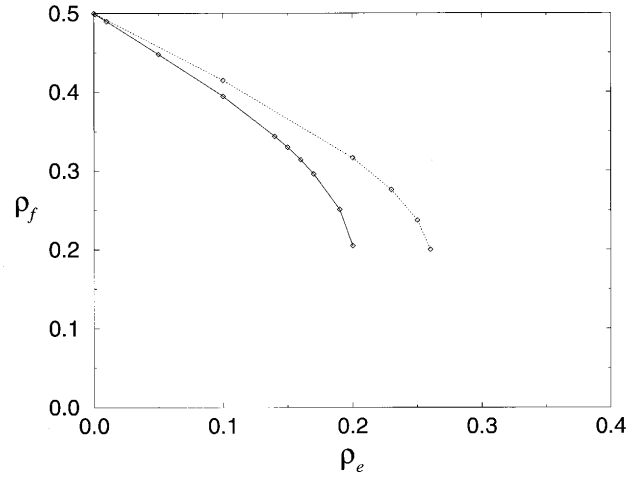

FIG. 6. The order parameter fire density ρ_f as function of the density of empty sites ρ_e in one dimension (—, nearest-neighbor interaction; . . . , the fire is allowed to jump over one empty site if necessary). For $\rho_e > \rho_e^{c,4} \approx 0.2$ and $\rho_e > \rho_e^{c,4} \approx 0.26$, respectively, the fire dies out. In the reverse direction, ρ_f remains zero until $\rho_e = \rho_e^{c,1} = 0$.

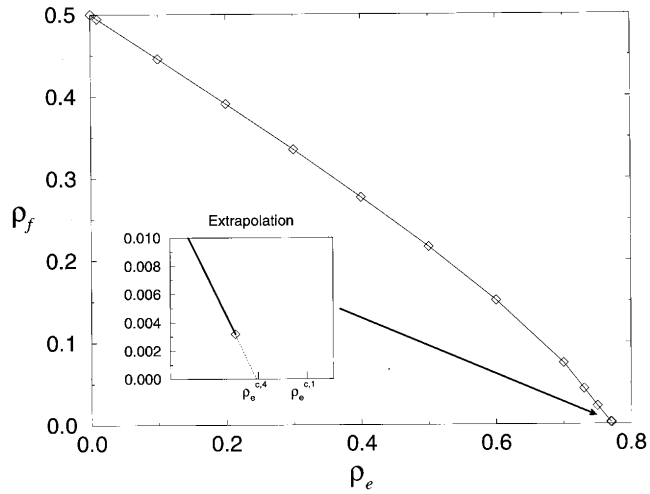

FIG. 7. The order parameter fire density ρ_f as function of the density of empty sites ρ_e in three dimensions. The extrapolation of the fire curve yields the critical density $\rho_e^{c,4} \approx 77.1\% \pm 0.2\%$.

versa. Strings of more than two trees or fires are not stable, since sooner or later they would be invaded by fires. The stationary state is periodic with period 2. The introduction of empty sites makes the automaton nondeterministic, because the trees can now choose where to grow. This variant has not been investigated so far. In the simulations, system sizes of up to $L = 10^7$ were used. The measured order parameter curves for the one-dimensional case can be seen in Fig. 6. In addition to the usual nearest-neighbor interaction, we simulated also a variant where the fire is allowed to jump over one empty site if necessary. The curves start linearly at $\rho_f = \rho_t = 1/2$ with different slopes (for an explanation see the Appendix). For increasing ρ_e one observes the same phenomena as in two dimensions. The tree clusters [strings in one dimension (1D)] become larger and are accompanied by fire on at least one of their ends. At $\rho_e = \rho_e^{c,4} \approx 20\%$ ($\rho_e^{c,4} \approx 26\%$ for next-nearest-neighbor interaction) the density of empty sites is too high for this structure to survive, and the fire density drops from a finite value of approximately 20% to zero, since the system does not have the possibility to rearrange itself into a spiral-wave phase. Instead, now isolated chunks of trees are ignited and burn down in finite time. In the reverse direction, ρ_f remains zero until $\rho_e = \rho_e^{c,1} = 0$, i.e., the hysteresis in one dimension is maximum. In the vicinity of the point $(\rho_e = 0, \rho_f = 0)$, the critical behavior of the SOC FFM in one dimension [20] is reproduced. Since there exists no spiral phase in one dimension, there are no $\rho_e^{c,2}$ and $\rho_e^{c,3}$.

The two-dimensional simulations were also done with a triangular lattice and yielded the same behavior as for the square lattice (for the order parameter curve see Fig. 3). The values of $\rho_e^{c,1,2,3,4}$ and the slope of the order parameter curve for $\rho_e \to 0$ of course are different (see Table I).

In three dimensions, we could identify a subcritical phase as well as a mixed phase. The order parameter curve is plotted in Fig. 7. Due to small L ($L \leqslant 300$) the critical exponents in the subcritical phase and the critical density $\rho_e^{c,1}$ could not be measured with sufficient accuracy. The mixed phase in three dimensions shows analogous behavior to the two-dimensional mixed phase and does not display new phenomena. The fire density curve could not be measured for very small ρ_f ($\rho_f \lesssim 0.2\%$), due to finite size effects. If one extrapolates the fire density curve to the point $\rho_f = 0$, one arrives at 77.3%, therefore, $\rho_e^{c,4}$ lies between the last simulated

TABLE I. The simulation results for various dimensions and lattice types. In the case 1D (*) the fire was allowed to jump over one empty site, if necessary.

Lattice type	1D	1D (*)	2D	2D triangular	3D
$\rho_e^{c,1}$	0%	0%	59.2(1)%	66.4(4)% [a]	78.1(1)%[a]
$\rho_e^{c,2}$	-	-	60.8(5)%	67.7(5)%	-
$\rho_e^{c,3}$	-	-	54.2%	61.7%	-
$\rho_e^{c,4}$	20%	26%	54.7%	62.2%	77.1(2)%
$-\left.\frac{\partial \rho_f}{\partial \rho_e}\right\|_{\rho_e=0}$	1.00(1)	0.85(1)	0.67(1)	0.54(1)	0.55(1)

[a]Taken from [8].

density 76.9% and 77.3%, i.e., $\rho_e^{c,4}=77.1\%\pm0.2\%$. The fact that there exists a gap between the end point of the critical phase $\rho_e^{c,1}\approx78.1\%$ (taken from [8]) and the end point of the mixed phase $\rho_e^{c,4}$ leaves open the possibility of the existence of a third phase containing the three-dimensional analogon of spiral waves (scroll waves). Due to the finite size of our sample, however, we could only observe two-dimensional, flat fire fronts in that region. The results for all simulated lattices and dimensions can be seen in Table I.

VIII. MAPPING SELF-ORGANIZED CRITICALITY ONTO CRITICALITY

The model we have investigated in this paper is an example of a system which is far from equilibrium. It shows a wealth of interesting structures depending on the density of empty sites ρ_e. For large ρ_e, we find a region of vanishing fire density which contains the critical behavior of the SOC forest-fire model. For lower density of empty sites we obtain the spiral waves of the Bak, Chen, and Tang [1] model. Finally, for even lower ρ_e, we find a phase in which the trees show the tendency to form clusters with the fire burning at their edges. The transition between the second and the third phase is of first order, whereas the transition between the first and the second phase is rather unconventional. We find hysteresis and critical behavior on only one side of the transition. The close relation of the spiral-wave phase with the synchronized phase of the model of [11] allows us to understand the mechanism which determines the density distribution in the spiral state of not only this model, but of arbitrary excitable systems. In particular, it yields the density in front of the excitation fronts, the minimum density of excitable constituents that is necessary to sustain the excitation, and the factor of proportionality between the distance of the spiral arms and the ''tree growth'' rate p.

Apart from being interesting in its own right, the model presented in this paper (like the model of [11]) has to be seen also in the context of the general claim of [12], that the critical points of SOC models can be regarded as ordinary critical points of second-order phase transitions. It was claimed in [12] that this should be possible for all SOC models. There were also given instructions on how to achieve this goal for some particular models, including the forest-fire model.

The results in this paper and in [11], however, disprove this hypothesis. While the subcritical side of the transition in both models behaves as expected, the other side (the side with a supposed nonvanishing order parameter) always exhibits surprising features. In the model of [11] we found a whole critical region and lots of first-order phase transitions, whereas the actual model shows hysteresis and no criticality at all.

Although these ''negative'' results cannot strictly rule out the possibility that for some further slight change of the rules one might succeed in obtaining the usual ''decent'' behavior of the order parameter, the argument at the end of Sec. IV, together with the simulation results of this paper and of [11] make it seem very unlikely. We consider it to be more probable that a subset of SOC models are ''only'' ordinary critical models ''in disguise.'' With these models the mapping proposed in [12] should be possible (the results in [21] also seem to point in that direction), while there also exist genuine SOC models for which this procedure cannot be carried through. The forest-fire model seems to belong to the second class.

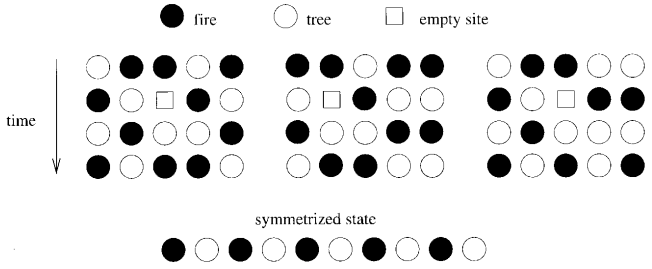

FIG. 8. The possible effects of the introduction of one empty site into a one-dimensional system at $\rho_e=0$.

We suggest that similar phenomena and difficulties (critical regions, hysteresis at the critical point, critical behavior on only one side) will also be found in other models of SOC, as, e.g., the sandpile, earthquake, and evolution models.

This work was supported by the Deutsche Forschungsgemeinschaft (DFG) under Contract No. Schw 348/7-1. We thank B. Drossel for fruitful discussions.

APPENDIX: SOME PROPERTIES OF THE ORDER PARAMETER CURVE

All order parameter curves considered in the previous sections started at the point $\rho_f=\rho_t=1/2,\rho_e=0$. This starting point is independent of dimension or lattice type, which can be seen as follows. For $\rho_e=0$ each tree will sooner or later be set on fire by one of its z nearest neighbors. Once having set the tree on fire, the fire jumps forever between this site and its neighbors, because its neighbors, after burning down, have to become trees again in the next time step (there are no empty sites). The dynamics of these $1+z$ sites then is fixed. After each time step trees and fires change places. But the fire can still propagate to other sites, so that finally the whole system consists of such ''blinking'' regions. The state is periodic with period 2 and the average fire and tree densities have to be 1/2. For a random initial state the densities are 1/2 also without averaging.

The slope of $\rho_f(\rho_e)$ for $\rho_e\to0$ depends only on the number of nearest neighbors z and lies always within the interval $[-1;-1/2]$. This can be seen as follows. If one takes a stationary state at $\rho_e=0$ and inserts some empty sites by removing an equal number of trees and fires, the system will not remain in this state (with a slope of $-1/2$), but will adjust itself to a new stationary state with an even lower number of fires, since the spreading conditions for the fire are now worse than before due to the inserted empty sites. The magnitude of this effect depends only on the coordination number z. The larger is z, the smaller is the effect. On an infinite-dimensional lattice, the fire density will not readjust itself at all, because no fire can feel the empty sites. The slope in this case is the maximum possible slope $-1/2$. This can also be seen mathematically. All fires have been trees in the preceding time step, therefore $\rho_f\leqslant\rho_t$ in the stationary

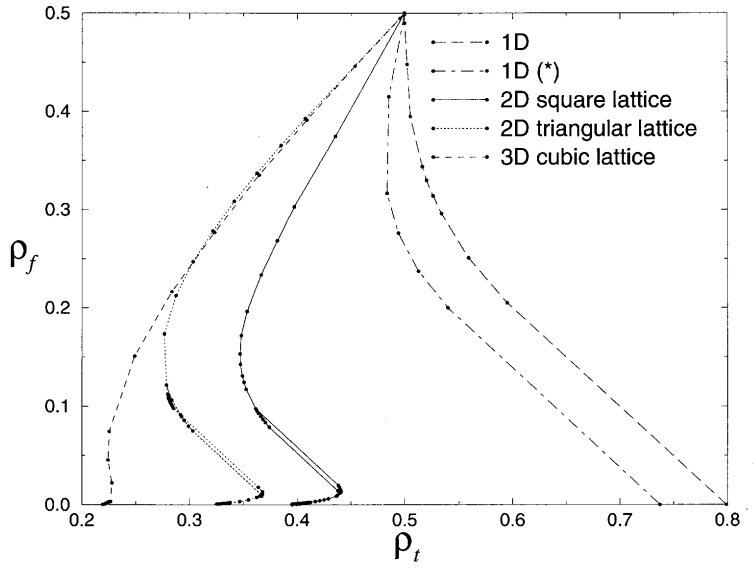

FIG. 9. The order parameter fire density ρ_f for all simulated dimensions and lattice types as function of the tree density ρ_t. In the case 1D (*) the fire was allowed to jump over one empty site, if necessary.

state. With $\rho_f+\rho_e+\rho_t=1$ it follows $\rho_f \leqslant 1/2-\rho_e/2$. Since for $\rho_e=0$ both sides of the last inequality are identical, one can differentiate and finds $\partial\rho_f/\partial\rho_e|_{\rho_e=0} \leqslant -1/2$. 1/2 is the upper bound for the slope.

The lower bound for the slope equals -1. This value is assumed for one dimension, as will be shown in the following by considering the effect of introducing one empty site into the stationary 1D state at $\rho_e=0$. Since the one-dimensional lattice has the smallest possible number of neighbors, its slope represents the lower bound. As argued in Sec. VII, in the one-dimensional stationary state at $\rho_e=0$ no more than two neighboring sites can be in the same state. In a symmetric state, where both neighbors of a tree are fires and vice versa, i.e., where fires and trees are strictly alternating, an empty site does not modify its neighborhood. Since the effects of the empty site are only local, it is sufficient to consider only three cases: One pair of sites in the same state (see the left part of Fig. 8), collision of two pairs (see the middle part of Fig. 8), and annihilation of two pairs (see the right part of Fig. 8). The possibilities of placing the empty site in these cases can be further reduced to the cases shown in the second line of Fig. 8. The reason is that, since in each time step n trees burn down and are refilled into $n+1$ empty sites, with probability ≈ 1 for large n the empty site at time t was a fire at time $t-1$, i.e., at time t the empty site occupies a place which would have been a tree in the unperturbed state. Therefore, we place the empty site at a tree site in the second line of Fig. 8. If instead we had chosen the neighboring tree sites, we would only have generated mirror-symmetric forms of the configurations shown. In the third line the empty site has disappeared from our small section of the system and has become a tree with probability ≈ 1 for $n \gg 1$. In the left case, the pair of sites moves one lattice spacing due to the presence of the empty site. In the middle case, two pairs which are separated by only one lattice site collide due to an empty site. In the right case, an empty site causes two neighboring pairs (which may have collided earlier) to annihilate each other and thereby symmetrize the region around the empty site. Therefore, sooner or later all pairs will have annihilated, and the entire system (with the exception of the single empty site) is in the symmetrical state. This evolution to the symmetrized state was also observed in the simulations.

We can therefore restrict ourselves to consider the consequences of the introduction of empty sites into such a highly symmetrical state. This has the advantage that there is no need to consider the neighboring sites, because they are not affected. There are two possibilities to introduce an empty site. The first one is to remove a tree. In the next time step this tree would have become a fire which it cannot do now. Instead, with very high probability a new tree is grown at this empty site. During the regrowth of trees the empty site effectively moves to another site in the system (which would have been a ''tree site''). While there is one excess tree in one part of the system, there is one tree less in another part of the system, so the total number of trees does not change. The number of fires, however, has decreased by one, since we prevented the ''birth'' of one fire. The second possibility is to remove a fire initially. If that happens, the empty site will have moved after the tree-growth phase to a ''tree site,'' and we have the first case again. Therefore, in each case the introduction of empty sites takes place completely at the expense of fire sites and $\partial\rho_f/\partial\rho_e|_{\rho_e=0}=-1$.

The measured results for the slope of the order parameter curve are shown in Table I. One can see that the slopes of the two-dimensional triangular lattice and the three-dimensional hypercubic lattice are the same, since they have the same coordination number $z=6$.

As mentioned earlier, not all tree densities between 0 and 1 are possible in the stationary state. If one transforms the $\rho_f(\rho_e)$ curves to $\rho_f(\rho_t)$ curves via $\rho_f+\rho_t+\rho_e=1$, one can read off the diagram the allowed ρ_t values (see Fig. 9). For these values it is possible to simulate the model with fixed ρ_t. The results do not differ from the results with fixed ρ_e. Also in this case, one has to be careful with the initial conditions, since there are sometimes two stationary states for the same value of ρ_t, and the initial state determines which of the two possible stationary states will be chosen by the system.

[1] P. Bak, K. Chen, and C. Tang, Phys. Lett. A **147**, 297 (1990).
[2] P. Grassberger and H. Kantz, J. Stat. Phys. **63**, 685 (1991).
[3] W. Moβner, B. Drossel, and F. Schwabl, Physica A **190**, 205 (1992).
[4] B. Drossel and F. Schwabl, Phys. Rev. Lett. **69**, 1629 (1992).
[5] C. L. Henley, Phys. Rev. Lett. **71**, 2741 (1993).
[6] P. Grassberger, J. Phys. A **26**, 2081 (1993).
[7] K. Christensen, H. Flyvberg, and Z. Olami, Phys. Rev. Lett. **71**, 2737 (1993).
[8] S. Clar, B. Drossel, and F. Schwabl, Phys. Rev. E **50**, 1009 (1994).
[9] J. J. Tyson and J. P. Keener, Physica D **32**, 327 (1988).
[10] E. Meron, Phys. Rep. **218**, 1 (1992).
[11] S. Clar, B. Drossel, and F. Schwabl, Phys. Rev. Lett. **75**, 2722 (1995).
[12] D. Sornette, A. Johansen, and I. Dornic, J. Phys. (France) I **5**, 325 (1995).
[13] D. Stauffer and A. Aharony, *Introduction to Percolation Theory* (Taylor and Francis, London, 1992).
[14] S. Clar, B. Drossel, K. Schenk, and F. Schwabl (unpublished).
[15] B. Drossel and F. Schwabl, Physica A **199**, 183 (1993).
[16] J. Ross, S. C. Müller, and C. Vidal, Science **240**, 460 (1988).
[17] J. M. Davidenko, A. V. Pertsov, R. Salomonsz, W. Baxter, and J. Jalife, Nature (London) **355**, 349 (1992).
[18] K. J. Lee, E. C. Cox, and R. E. Goldstein, Phys. Rev. Lett. **76**, 1174 (1996).
[19] S. Wolfram, Rev. Mod. Phys. **55**, 601 (1983).
[20] B. Drossel, S. Clar, and F. Schwabl, Phys. Rev. Lett. **71**, 3739 (1993).
[21] F. Bagnoli, P. Palmerini, and R. Rechtman (unpublished).